Available online at www.sciencedirect.com
SCIENCE DIRECT®
International Journal of Pharmaceutics 302 (2005) 1–9
international journal of pharmaceutics
www.elsevier.com/locate/ijpharm

Mechanisms of formation and disintegration of alginate beads obtained by prilling

Pasquale Del Gaudio *, Paolo Colombo, Gaia Colombo, Paola Russo, Fabio Sonvico

Department of Pharmacy, University of Parma, I-43100 Parma, Italy

Received 6 October 2004; received in revised form 4 May 2005; accepted 19 May 2005
Available online 15 August 2005

Abstract

In this paper, compendial sodium alginate beads have been manufactured by laminar jet break-up technology. The effect of polymer concentration, viscosity and polymeric solution flow rate on the characteristics of beads was studied. Size distribution of alginate beads in the hydrated state was strongly dependent on the flow rate and viscosity of polymer solutions, since a transition from laminar jet break-up conditions to vibration-assisted dripping was observed. The re-hydration kinetics of dried beads in simulated gastric fluid (SGF) showed that the maximum swelling of beads was reached after 1–2 h, with an increase in volume of two to three times and a time lag dependent on the polymer concentration. The re-hydration swelling profiles in simulated intestinal fluid (SIF) showed no time lag and higher swelling volume; moreover, in this medium after the maximum swelling was reached, the bead structure was quickly disaggregated because of the presence in the medium of phosphate able to capture calcium ions present in the alginate gel structure.
© 2005 Elsevier B.V. All rights reserved.

Keywords: Alginate beads; Laminar jet break-up; Prilling; Controlled drug release

1. Introduction

The need to control drug release or to overcome drug stability problems in oral delivery has been a stimulus for the development of microencapsulated products. Several physical methods for microencapsulation such as spray drying, fluid bed coating, electrostatic deposition or extrusion have been investigated for the manufacturing of particles of controlled dimension and morphology. In the last few years, the technique known as laminar jet break-up or prilling has raised considerable interest because of the possibility to obtain microparticles for drug delivery of a narrow dimensional range and high encapsulation efficiency (Sakai and Hoshino, 1980; Matsumoto et al., 1986; Brandenberg and Widmer, 1998). These microparticles or beads are produced by breaking apart a laminar jet of polymer solution into a row of mono-sized drops by means

* Corresponding author. Tel.: +39 0521 905088; fax: +39 0521 905006.
E-mail address: delgaudi@nemo.cce.unipr.it (P. Del Gaudio).

0378-5173/$ – see front matter © 2005 Elsevier B.V. All rights reserved.
doi:10.1016/j.ijpharm.2005.05.041

of a vibrating nozzle device. The resultant droplets fall into a polymer gelation solution in which they are solidified as beads. This technique has shown attractive applications in different fields, including cell immobilization, owing to its mild operative conditions (Hunik and Tramper, 1993; Brandenberg and Widmer, 1998; Serp et al., 2000; Koch et al., 2003).

Sodium alginate is a biodegradable and bioadhesive polymer. Some pharmacopoeia monographs are devoted to this polysaccharide, stating the quality requirements for its application in pharmaceutical preparations (Fundueanu et al., 1999; Koch et al., 2003). Since sodium alginate is capable of producing beads by ionotropic gelation in the presence of bivalent cations, it has frequently been proposed for encapsulating drugs and biological materials (Orive et al., 2002; Ueng et al., 2004).

Several papers can be found in the literature on the use of sodium alginate for bead production (Thu et al., 1996; Kikuchi and Okano, 2002; Schwinger et al., 2002; Tonnesen and Karlsen, 2002; Koyama and Seki, 2004). The sodium alginate used in these studies was of a narrow range molecular weight with a well-characterized viscosity. No paper reports the use of pharmacopoeia-grade sodium alginate for the manufacturing of beads.

The aim of this work was to study the effects of relevant process variables on the characteristics of compendial sodium alginate beads manufactured by laminar jet break-up technology. In particular, polymer concentration, solution viscosity and jet flow rate were considered. The objectives of the present work were to identify the mechanisms of formation and disintegration of alginate beads obtained by prilling.

2. Materials and methods

Sodium alginate European Pharmacopoeia 4 (Carlo Erba, Milan, Italy) was used as purchased, without further purification. Water content (5%, w/w) was determined by thermo-gravimetric analysis (TG50-Mettler Toledo, Columbus, OH, USA). The viscosity of sodium alginate solutions was measured by rotational rheometer (Bohlin Instruments Division, UK) where a cone–plate combination (CP 4/40) was used as measuring system.

Sodium alginate solution density was determined by glass picnometer in accordance with Ph. Eur. 4 (DISA, Milan, Italy).

$CaCl_2$ anhydrous, granular (MERCK, Darmstadt, Germany).

2.1. Bead preparation

An appropriate amount of sodium alginate was dissolved in distilled water at 20–22 °C under gentle stirring for 18 h in order to obtain 50 ml of solution with concentrations ranging between 0.5 and 2.75% (w/w). The solution was then thermostated at 25 °C and beads were manufactured by a vibrating nozzle device (Nisco Encapsulator Unit, Var D; Nisco Engineering Inc., Zurich, CH), equipped with a syringe (Model 200 Series, Kd Scientific Inc., Boston, MA, USA) pumping the solution through the nozzle. The experiments were performed at different volumetric flow rates, namely 10, 15 and 20 ml/min. The vibration frequency used to break up the liquid jet was set at 250 Hz, amplitude 100% and the nozzle diameter was 400 μm. A stroboscopic lamp was set at the same amplitude as the frequency used for the nozzle, in order to visualize the falling droplets. The droplets fell into a 0.5 M $CaCl_2$ solution, where they were gelified under gentle stirring. The distance between the vibrating nozzle and the gelling bath was fixed at 25 cm. The holding time inside the $CaCl_2$ solution was set at 4 h. The beads were then recovered and rinsed thoroughly with distilled water. Finally, the beads were dried at room temperature by exposure to air (22 °C; 67% RH) for several hours until constant weight was reached.

2.2. Bead size and morphology

Hydrated and dried bead size distribution were measured by optical microscopy (Citoval 2, Alessandrini, Modena, Italy). Pictures were taken with a video camera (CCD-1, JVC, Tokyo, Japan) attached to the microscope. The projection diameter was obtained by image analysis (Image J Software, Wayne Rasband, National Institute of Health, Bethesda, MD, USA). At least 75 microparticle images were analyzed for each preparation and the length-number mean diameter was calculated. The average of mean diameters and relative standard deviations were calculated for at least three different jet break-up processes.

The perimeter and projection surface area obtained by image analysis were used to calculate a sphericity coefficient (SC) by the following equation (Almeida-Prieto et al., 2004):

$$SC = \frac{4\pi A}{P^2}$$

where A is the bead surface area and P its perimeter.

Scanning electron microscopy was performed on dried beads using a Jeol 6400 microscope (Jeol, Tokyo, Japan) on a deposition of a 200–400 Å thick carbon layer. Analysis was conducted at 15 keV and the magnification was ×100. A fractal descriptor of the bead roughness was calculated from grey level distribution analysis measured on the SEM images of the beads. The images were taken at the same magnification and a scanned area of the SEM image, a box of 200 μm width and 200 μm length was analyzed by Image J Software using the algorithm known as the "box counting method" (Chappard et al., 2003; Ferrari et al., 2004). The analysis was carried out on five different area sections for each bead image considered and a mean fractal descriptor was obtained. The analysis was repeated on at least 10 beads for each batch.

2.3. Swelling kinetics of dried beads

Swelling experiments were performed in simulated gastric fluid (SGF), simulated intestinal fluid (SIF) (USP 27) without enzymes and Tris buffer (Trizma® hydrochloride, Sigma–Aldrich, St. Louis MO, USA). Dried beads were placed in a vessel containing the selected buffer under gentle magnetic stirring; then, using an optical microscope equipped with a video camera, the bead volume was measured during swelling at different times and compared with the volume in dry state. The degree of swelling, or swelling ratio, was calculated as the ratio between the bead volume in swollen and dry states.

3. Results and discussion

3.1. Effect of sodium alginate concentration and viscosity on hydrated bead micromeritics

The effects of concentration, viscosity and volumetric flow rate of the sodium alginate solution on bead micromeritics were studied. A first series of prilling experiments was performed, in accordance with literature data (Schneider and Hendriks, 1964; Sakai et al., 1985), in operating conditions inducing the jet break-up of a sodium alginate solution at 0.5% (w/w). Thus, beads from sodium alginate solutions at different concentrations from 0.5 to 2.75% (w/w) were produced using the nozzle of 400 μm vibrating at 250 Hz with a volumetric solution rate of 10 ml/min. The gelation time in the Ca^{2+} solution was 4 h.

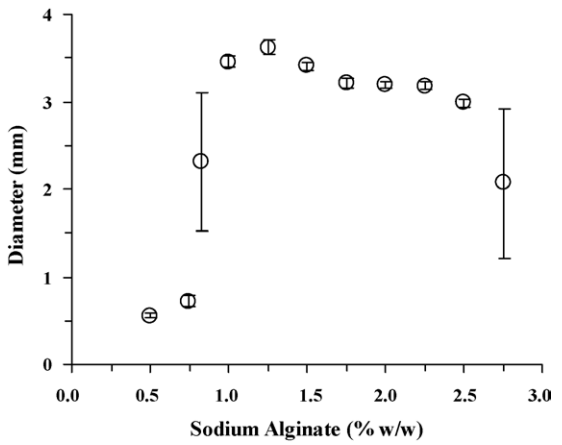

Fig. 1. Average of mean diameters and standard deviations of hydrated beads plotted against sodium alginate concentration (n = 3–5).

The mean diameter of beads produced in these conditions was measured and plotted against sodium alginate concentration (Fig. 1). Using the compendial sodium alginate solutions of a concentration lower than 0.85% (w/w), hydrated beads of a projection diameter lower than 1 mm were obtained. When the concentration of alginate was increased to above 0.85 (w/w), a sudden augmentation of bead size to around 3 mm was observed. Thereafter, this bead diameter remained almost constant despite the further increase in polymer concentration to 2.5% (w/w). Above this value, the beads were difficult to produce, and with a solution of 3% (w/w) sodium alginate the prilling apparatus in the selected conditions was not able to break up the polymer solution jet into droplets. Two points characterized by very high variability of bead mean size were observed in correspondence to 0.85 and 2.75% (w/w) sodium alginate solutions, respectively. This variability in size distribution was due to the generation of a

bimodal population of beads, determined by an alteration in the jet break-up during the prilling experiments. These two concentration values delimitated a region in which the beads had a large size with a narrow distribution.

The shape of the beads was assessed by means of a sphericity coefficient, i.e. the ratio between the projected area of the bead and the square of its perimeter. The beads were almost spherical, since we measured values always higher than 0.95 (1 corresponding to a sphere), independently of sodium alginate concentration.

The bead size distribution was then studied in terms of sodium alginate solution density, surface tension, viscosity and volumetric flow rate. In the range of concentration between 0.5 and 3.0% (w/w), the density of the alginate solutions increased linearly from 1.002 to 1.013 g/cm^3. In the same range, the surface tension remained fairly constant up to 0.85% (w/w), and then increased linearly up to 2.75% (w/w) (Fig. 2). Rheological measurements were performed on the alginate solutions in order to determine the viscosity in correspondence to the nozzle. Since sodium alginate solutions showed pseudoplastic behaviour, the rheological data were analyzed using the following Cross equation (Soong and Shen, 1981):

$$\frac{\mu - \mu_0}{\mu_0 - \mu_\infty} = \frac{1}{1 + (c\dot{\gamma})^n}$$

where μ is the viscosity at the shear rate applied to the solutions inside the nozzle, μ_0 and μ_∞ the viscosity

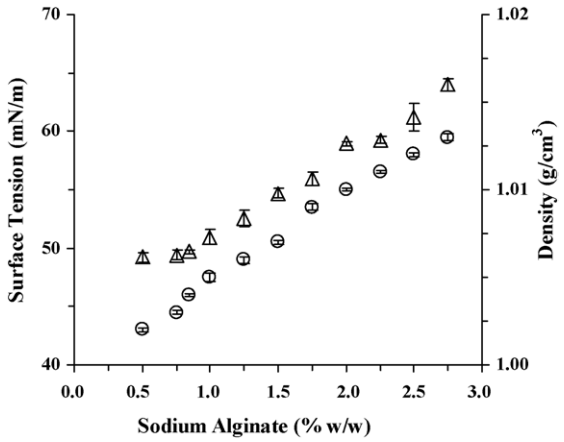

Fig. 2. Relationship between sodium alginate concentration and solution surface tension (△) and viscosity at the nozzle (◯) (mean ± S.D.; $n = 3$).

extrapolated at zero and infinite shear rates, respectively, and c and n are rheological parameters. The shear rate at the nozzle, $\dot{\gamma}$, can be determined by knowing the solution volumetric flow rate Q (m^3/s) and the nozzle radius r (m) according to the following equation:

$$\dot{\gamma} = \frac{4Q}{r^3\pi}$$

This value allows us to calculate the viscosity at the nozzle.

Moreover, in order to assess that the jet flow inside the nozzle was laminar, the Reynolds number, *Re*, in the case of a solution circulating in a tube, was calculated

Table 1
Rheological parameters obtained by Cross equation (μ_0, viscosity at zero shear rate; μ_∞, viscosity at infinite shear rate; μ, viscosity at the nozzle; c and n, rheological coefficients) and Reynolds number (*Re*) for sodium alginate solutions at a flow rate of 10 ml/min (mean ± S.D.; $n = 3$)

Sodium alginate (%, w/w)	$c(s)$ ($\times 10^{-3}$)	n	μ_0 (mPa)	μ_∞ (mPa)	μ (mPa)	*Re*
0.50	1.4 ± 0.2	0.59 ± 0.03	101 ± 4.7	16 ± 1.2	25 ± 1.3	21
0.75	2.6 ± 0.2	0.68 ± 0.03	143 ± 4.8	21 ± 1.4	28 ± 1.7	19
0.851	2.6 ± 0.2	0.70 ± 0.04	162 ± 5.2	28 ± 2.2	35 ± 2.5	15
1.00	2.9 ± 0.2	0.74 ± 0.05	197 ± 6.3	36 ± 3.7	42 ± 3.9	13
1.25	3.8 ± 0.3	0.88 ± 0.04	291 ± 6.3	46 ± 5.7	51 ± 6.1	11
1.50	4.3 ± 0.3	0.97 ± 0.04	375 ± 9.8	66 ± 7.6	68 ± 7.2	8
1.75	5.3 ± 0.3	1.13 ± 0.04	551 ± 9.9	112 ± 10.1	113 ± 9.3	5
2.00	6.0 ± 0.3	1.20 ± 0.03	779 ± 11.2	159 ± 9.6	160 ± 10.1	3
2.25	6.4 ± 0.4	1.42 ± 0.04	1127 ± 35.3	249 ± 10.2	250 ± 10.7	2
2.50	6.7 ± 0.5	1.63 ± 0.05	1502 ± 59.1	352 ± 12.8	353 ± 14.4	1
2.75	6.8 ± 0.6	1.91 ± 0.07	1892 ± 92.5	471 ± 19.1	471 ± 20.2	1
3.00	6.9 ± 0.6	2.10 ± 0.07	2937 ± 95.4	721 ± 20.5	721 ± 20.6	1

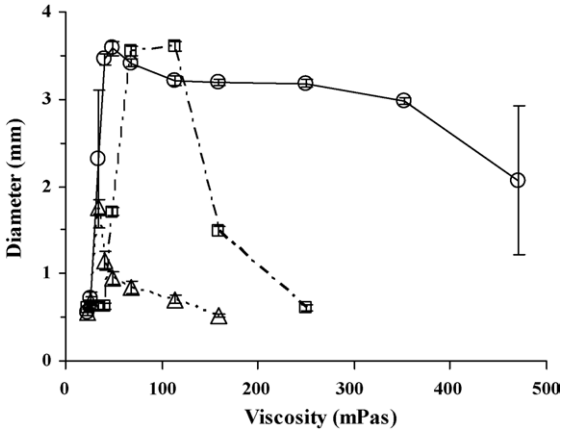

Fig. 3. Relationship between viscosity at the nozzle and the average mean projection diameters of hydrated beads obtained with a jet flow rate of (◯) 10 ml/min, (□) 15 ml/min and (△) 20 ml/min (mean ± S.D.; $n = 3$).

according to the following equation:

$$Re = \frac{\rho \upsilon d}{\mu}$$

where ρ is the solution density, υ (m/s) the jet velocity of polymer solution, d the nozzle diameter and μ is the viscosity at the nozzle. The flow is laminar if $Re < 2000$ (Dumas et al., 1992). In Table 1, the rheological parameters of the Cross equation, the viscosity at the nozzle and the Reynolds number for the solutions having different sodium alginate concentrations are reported. Since all the solutions exhibited a Reynolds number much lower than 2000, the flow inside the nozzle was considered as being laminar. At each concentration, the viscosity at the nozzle was lower than the viscosity at zero shear rate and close to the infinite viscosity (see Table 1). At zero shear rate, compendial alginate solutions showed low viscosity values (<200 mPa) (Orive et al., 2002) when the concentration was less than 1% (w/w); on increasing the concentration, the viscosity exhibited exponentially increasing values. However, owing to the viscoelastic behaviour, the viscosity at nozzle shear rate resulted as being lower than 100 mPa for 1.5% (w/w) sodium alginate solution and increased 10 times when the concentration was doubled.

The size of beads produced at 10 ml/min was plotted against viscosity at the nozzle of alginate solutions (Fig. 3). In the selected conditions, solutions of sodium alginate generated beads of a small diameter (<750 μm) when viscosity was lower than 30 mPa, whereas solutions exhibiting viscosity from 40 to 350 mPa produced large beads (3000–3500 μm). Using the stroboscopic lamp, we were able to observe, in the case of solutions having a viscosity lower than 35 mPa, a smooth jet of liquid exiting from the nozzle that was effectively broken by vibration into droplets whose size was in the expected range for a nozzle of 400 μm (Sakai et al., 1985). However, when the viscosity was higher than 35 mPa, the solution showed a tendency to adhere to the nozzle, transforming the smooth jet exiting from the nozzle into a dripping regime, i.e. a sequence of large drops even in the absence of the nozzle vibration (Sakai and Hoshino, 1980). The bimodal size distribution of beads observed at 35 mPa was the indication of the transition from a smooth jet of the liquid to dripping regimes. In addition, when the viscosity at the nozzle reached 400 mPa, bead populations having a bimodal size distribution were produced. With this high viscosity solution, we again observed the formation of a smooth jet of the liquid, although the vibration imposed was not able to break up the jet into droplets.

In conclusion, at a flow rate of 10 ml/min, beads having a large size and a narrow distribution were obtained from a 400 μm nozzle vibrating at 250 Hz using solutions of a viscosity between 40 and 350 mPa. However, in these conditions the manufacturing process was not jet break-up but that of a dripping solution assisted by nozzle vibration. The absence of vibration produced beads of a larger size and a broader distribution. Uniform small size beads of sodium alginate could also be obtained at nozzle viscosity values lower than 35 mPa, where the manufacturing conditions were laminar jet break-up. Finally, the bead size distribution was found to be bimodal in correspondence to the transition from smooth jet to dripping regimes. Sodium alginate solutions of a viscosity higher than 400 mPa could not be used for bead production in these operating conditions.

In successive series of prilling experiments, the volumetric flow rate was raised to 15 ml/min and 20 ml/min. The increase in the flow rate did not significantly affect the viscosity at the nozzle, given that the values at the nozzle were close to infinite viscosity. However, the increase in the flow rate affected the transition between the jet break-up and dripping process. At 15 ml/min, the formation of beads by dripping was observed between 68 and 113 mPa, whereas outside this range the formation was under jet break-up control.

At 20 ml/min, beads were manufactured exclusively by the jet break-up process. Therefore, the increased volumetric flow rate prevented the adhesion of the alginate solution to the nozzle, avoiding the change to liquid jet flow regime. For the viscosity values investigated, no bimodal particle size distribution was observed at higher jet rates. Additionally, the viscosity values at which beads could not be produced decreased with the increased flow rate. In fact, the prilling vibration at 250 Hz was unable to break up the solution jet when the nozzle viscosity was higher than 250 and 180 mPa for 15 and 20 ml/min of flow rate, respectively.

3.2. Dried beads

The beads were dried by exposure to air in normal conditions of temperature and humidity. The residual water content of dried beads was $18 \pm 1.3\%$ for the highest alginate concentration and $12 \pm 1.2\%$ (w/w) for the lowest concentration. The volume of the dried beads was found to be between 35 and 20% for the highest and lowest alginate concentrations, respectively.

The surface roughness of dried beads was quantified by fractal analysis, where the fractal descriptor value ranged between 1 and 2, 1 being for a smooth surface. The dried bead surface exhibited roughness values decreasing from 1.30 to 1.08 with the increasing of the sodium alginate concentration, as shown in the graph of Fig. 4. Therefore, the increase in the amount of sodium alginate in the solution produced smoother beads, as shown in Fig. 5, where beads manufactured at two different sodium alginate concentrations are exposed.

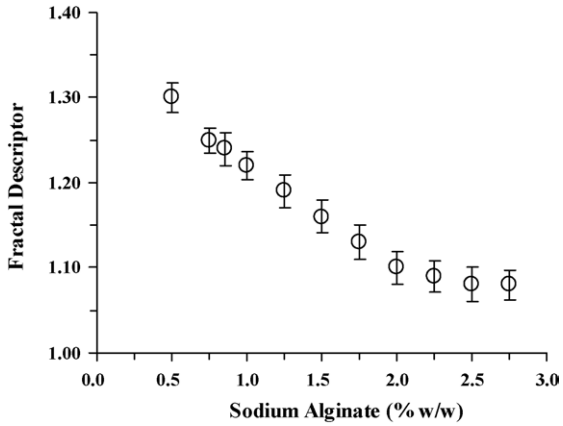

Fig. 4. Relationship between the fractal dimension of the beads and the concentration of the sodium alginate solutions (mean ± S.D.; $n = 5$).

The release of any encapsulated drug or biological material from dried beads requires a re-hydration process. For this reason, swelling experiments were carried out in simulated gastric fluid pH 1.2 and simulated intestinal fluid pH 6.8 (USP 27) without enzymes, to study the re-hydration kinetics of beads produced from solutions having different concentrations in sodium alginate. Three batches of beads were tested, namely beads prepared from 0.75, 1.5 and 2.5% (w/w) solutions at a volumetric flow rate of 10 ml/min. As shown in Fig. 6, in SGF the maximum swelling of beads was reached after 1–2 h, with an increase in the dried bead volume of two to three times depending on the polymer concentration. The maximum swelling val-

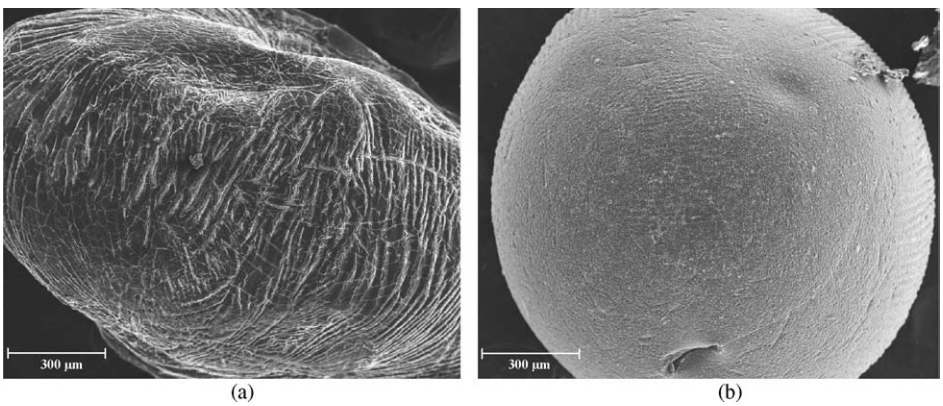

(a) (b)

Fig. 5. Dried sodium alginate beads obtained from solutions at different concentrations: (a) 1.0% (w/w) and (b) 2.0% (w/w).

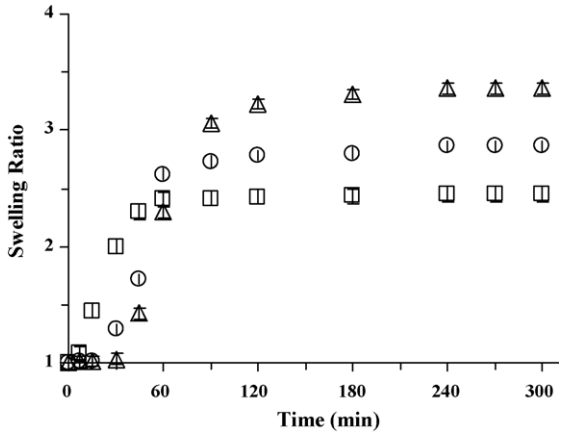

Fig. 6. Swelling process of dried beads of sodium alginate in SGF without enzymes. (□) 0.75% (w/w), (◯) 1.5% (w/w) and (△) 2.5% (w/w) (mean ± S.D.; $n = 3$).

ues remained constant until the end of the experiment (48 h). Moreover, a time lag was present in each swelling profile. This time lag was longer as polymer concentration increased. However, in these conditions the final volume of the re-hydrated beads was still lower than the original volume of the hydrated beads (Yotsuyanagi et al., 1987, 1991; Fundueanu et al., 1999).

The swelling profiles in SIF pH 6.8 revealed no time lag (even for beads prepared with high concentrated sodium alginate solutions) and a higher swelling ratio. In Fig. 7, the behaviour of the beads produced

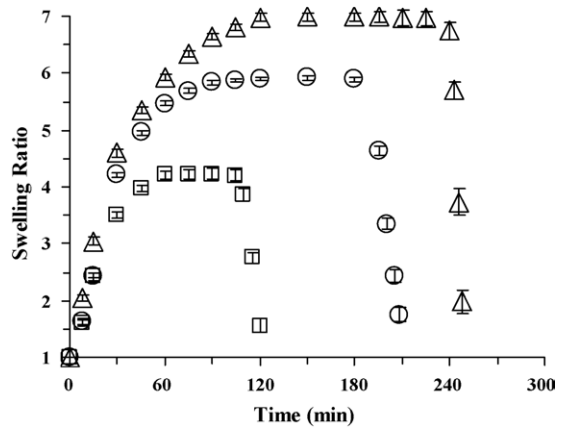

Fig. 7. Swelling profiles of dried beads in SIF without enzymes. (□) 0.75% (w/w), (◯) 1.5% (w/w) and (△) 2.5% (w/w) (mean ± S.D.; $n = 3$).

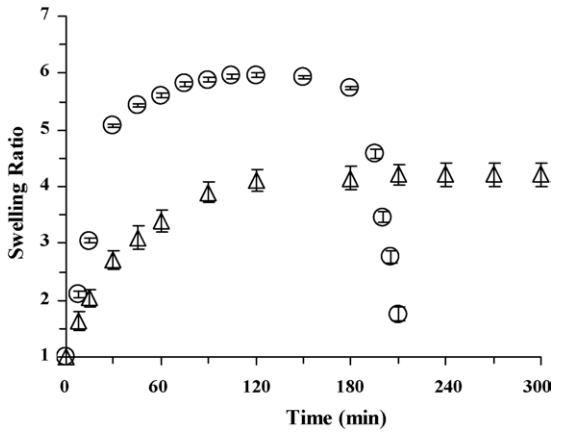

Fig. 8. Swelling profiles of dried beads of sodium alginate. (△) 1.5% (w/w) in Tris buffer pH = 6.8 and (◯) 1.5% (w/w) in Tris buffer plus EDTA pH = 6.8 (mean ± S.D.; $n = 3$).

from the 0.75, 1.5 and 2.5% (w/w) alginate solutions is shown. In this medium, the maximum swelling volume reached was higher than the volume of hydrated beads before drying. This phenomenon has also been observed by other authors (Yotsuyanagi et al., 1991; Bajpai and Sharma, 2004). The maximum swelling ratio was dependent on the sodium alginate concentration: in fact, it was close to 4 for the 0.75% (w/w) solution, around 6 for the 1.5% (w/w) solution and 7 for the 2.5% (w/w) solution. In addition, the time of maximum swelling attainment was increased from 2 to 4 h by increasing the alginate concentration. Subsequently, the bead structure was quickly disaggregated, leading to the dissolution of the swollen bead. This peculiar swelling behaviour was attributed to the capturing of the calcium ions by phosphate ions contained in SIF buffer. In order to demonstrate this mechanism, swelling experiments on beads prepared from 1.5% (w/w) solution were performed in pH 6.8 Tris buffer. In this buffer, the swelling equilibrium was not followed by disaggregation/dissolution, since the beads remained coherent for more than 48 h (Fig. 8). Furthermore, the bead volume reached a maximum value that was lower than that exhibited in SIF buffer at the same pH, but corresponding to the bead volume before drying. Thus, we decided to perform swelling experiments with pH 6.8 Tris buffer to which EDTA, a chelating Ca^{2+} agent, was added. The results obtained, reproduced in Fig. 8, show that the profile of swelling ratio versus time was similar to the

one obtained in pH 6.8 SIF buffer: the same maximum volume followed by disaggregation/dissolution of the bead was obtained. Hence, the swelling kinetics of dried beads in the presence of a calcium capturing agent depended on the progressive displacement of calcium ions within the beads. This mechanism explained the swelling volume larger than that of the original hydrated beads and the disintegration of the bead structure when the maximum swelling was reached.

4. Conclusions

Using solutions of compendial sodium alginate and the selected jet break-up operating conditions, we found that the beads are produced according to two different mechanisms depending on the solution properties (viscosity, density and surface activity) and jet rate. In particular, large beads were manufactured when the formation mechanism was dripping assisted by vibration. In contrast, when the mechanism was laminar solution jet break-up, the size of beads was small. Both flow regimes, i.e. laminar jet break-up and vibration-assisted dripping, were able to produce beads of a narrow particle size distribution. Two specific values of solution viscosity resulted in the production of a bimodal population of beads at 10 ml/min in the conditions selected. These two values corresponded to the transition from the jet break-up to the dripping regime. By increasing the jet rate without modifying the nozzle vibration, we were able to limit the appearance of the dripping phenomenon, hence reducing the bead size.

A very interesting result of the research was the understanding of the swelling behaviour of the dried alginate beads during re-hydration at pH 6.8 when the buffer solution contained a Ca^{2+} capturing compound. In this situation, the beads re-hydrated to the maximum swelling volume in 2–4 h, depending on the concentration of the sodium alginate in the solution. The swollen mass then rapidly collapsed and dissolved. The mechanism involved in this swelling behaviour was calcium depletion from the bead structure. This phenomenon could be profitably used as a mechanism for controlling the release of diffusible drugs, but in particular for the delivery of biological material.

Acknowledgments

The authors would like to thank Professor C. Bonferoni and Professor Carla Caramella (University of Pavia) for their help in the rheological experiments.

References

Almeida-Prieto, S., Blanco-Mendez, J., Otero-Espinar, F.J., 2004. Image analysis of the shape of granulated powder grains. J. Pharm. Sci. 93, 621–634.

Bajpai, S.K., Sharma, S., 2004. Investigation of swelling/degradation behaviour of alginate beads crosslinked with Ca^{2+} and Ba^{2+} ions. React. Funct. Polym. 59, 129–140.

Brandenberg, H., Widmer, F., 1998. A new multinozzle encapsulation/immobilization system to produce uniform beads of alginate. J. Biotechnol. 63, 73–80.

Chappard, D., Degasne, I., Huré, G., Lagrand, E., Audran, M., Baslé, M.F., 2003. Image analysis measurement of roughness by texture and fractal analysis correlate with contact profilometry. Biomaterials 24, 1399–1407.

Dumas, H., Tardy, M., Rochat, M.H., Tayot, J.L., 1992. Prilling process applied to collagen solutions. Drug Dev. Ind. Pharm. 18, 1395–1409.

Ferrari, F., Cocconi, D., Bettini, R., Giordano, F., Santi, P., Tobyn, M., Pryce, R., Young, P., Caramella, C., Colombo, P., 2004. The surface roughness of lactose particles can be modulated by wet-smoothing using a high-shear mixer. AAPS PharmSciTech 5 (Article 60).

Fundueanu, G., Nastruzzi, C., Carpov, A., Desbrieres, J., Rinaudo, M., 1999. Physico-chemical characterization of Ca-alginate microparticles produced with different methods. Biomaterials 20, 1427–1435.

Hunik, J.H., Tramper, J., 1993. Large-scale production of kappa-carrageenan droplets for gel-bead production: theoretical and practical limitations of size and production rate. Biotechnol. Prog. 9, 186–192.

Kikuchi, A., Okano, T., 2002. Pulsatile drug release control using hydrogels. Adv. Drug Deliv. Rev. 54, 53–77.

Koch, S., Schwinger, C., Kressler, J., Heinzen, Ch., Rainov, N.G., 2003. Alginate encapsulation of genetically engineered mammalian cells: comparison of production devices, methods and microcapsule characteristics. J. Microencapsul. 20, 303–316.

Koyama, K., Seki, M., 2004. Cultivation of yeast and plant cells entrapped in the low-viscous liquid-core of an alginate membrane capsule prepared using polyethylene glycol. J. Biosci. Bioeng. 97, 67–72.

Matsumoto, S., Kobayashi, H., Takashima, Y., 1986. Production of monodispersed capsules. J. Microencapsul. 3, 25–31.

Orive, G., Ponce, S., Hernandez, R.M., Gascon, A.R., Igartua, M., Pedraz, J.L., 2002. Biocompatibility of microcapsules for cell immobilization elaborated with different type of alginates. Biomaterials 23, 3825–3831.

Sakai, T., Hoshino, N., 1980. Production of uniform droplets by longitudinal vibration of audio frequency. J. Chem. Eng. Jpn. 13, 263–268.

Sakai, T., Sadataka, M., Saito, M., Matsushita, K., 1985. Studies of disintegration of liquid column between production of uniform size droplets by vibration method. ICLASS-85 7B, 2–15.

Schneider, L.M., Hendriks, C.D., 1964. Source of uniform liquid droplets by vibration method. Rev. Sci. Instrum. 35, 1349–1350.

Schwinger, C., Koch, S., Jahnz, U., Wittlich, P., Rainov, N.G., Kressler, J., 2002. High throughput encapsulation of murine fibroblasts in alginate using the JetCutter technology. J. Microencapsul. 19, 273–280.

Serp, D., Cantana, E., Heinzen, C., Von Stockar, U., Marison, I.W., 2000. Characterization of an encapsulation device for the production of monodisperse alginate beads for cell immobilization. Biotechnol. Bioeng. 70, 41–53.

Soong, D., Shen, M., 1981. Kinetic network model for nonlinear viscoelastic properties of entangled monodisperse polymers. I. Steady state flow. J. Rheol. 25, 259–273.

Thu, B., Bruheim, P., Espevik, T., Smidsrod, O., Soon-Shiong, P., Skjak-Braek, G., 1996. Alginate polycation microcapsules. Some functional properties. Biomaterials 17, 1069–1079.

Tonnesen, H.H., Karlsen, J., 2002. Alginate in drug delivery systems. Drug Dev. Ind. Pharm. 28, 621–630.

Ueng, S.W., Yuan, L.J., Lee, N., Lin, S.S., Chan, E.C., Weng, J.H., 2004. In vivo study of biodegradable alginate antibiotic beads in rabbits. J. Orthop. Res. 22, 592–599.

Yotsuyanagi, T., Ohkubo, T., Ohhashi, T., Ikeda, K., 1987. Calcium-induced gelation of alginic acid and pH-sensitive reswelling of dried gels. Chem. Pharm. Bull. 35, 1555–1563.

Yotsuyanagi, T., Yoshioka, I., Segi, N., Ikeda, K., 1991. Acid-induced and calcium induced gelation of alginic acid: bead formation and pH-dependent swelling. Chem. Pharm. Bull. 39, 1072–1074.